J. King Saud Univ., Vol. 15, Science (2), pp. 81-101, Riyadh (A.H. *14223/23)*

Scaling Relations of Earthquake Parameters in the Red Sea Region

B. T. Punsalan and A.M. A9-Amri *Seismic Studies Center, King Saud University, Riyad, Saudi Arabia*

(Received *19/7/1422* H; accepted for publication *2611/1423 H)*

Abstract. Scaling relations for the attenuation of intensity and peak ground acceleration in terms of epicentral and hypocentral distances, surface-wave and body-wave magnitudes, and focal depth were preliminarily developed in the Red Sea region. The attenuation relations were determined empirically from homogeneous modeling of the modified isoseismal maps of earthquake events originating from different areas in the region, observed PGA data, and conversion of intensity to magnitude with focal depth.

The obtained scaling equations were generally expressed in the form: I = aiMi - bilog(D+Di) - ciD - dilog(h) + ei
I = aiMi - bilog(r/h) - ci(r-h) -dilog(h) + ei log(PGA) =
aiMi - bilog(D+Di) - ciD - dilog(h) + ei log(PGA) =
aiMi - bilog(r/h) - ci(r-h) - dilog(h) +ei

where the coefficients ai, bi, ci, di correspond to the type of magnitude, distance, auelastic attenuation coefficients; and focal depth respectively. Di is the approximate radius of perceptibility of the meizoseismal area corresponding to the type of attenuation coefficient, and ei the different constant terms. The findings can be considered as preliminary endeavors in providing the necessary means of estimating ground motion in the Red Sea region. The scaling relations could assist in the formulation of rational decision and strategies in environmental protection.

Introduction

Earthquakes are significant agent of natural disaster. A destructive earthquake leaves and causes a devastating impact to society and environment. Approximately 140,000 lives were lost from the 1923 Kwanto earthquake in Japan due to conflagration of fires and ground shaking [1]. Around 240,000 people were feared to have died from the 1976 Tangshan earthquake in China [2]. Several countries were adversely affected by the tsunami generated in the Chile earthquake of 1960 [3). The earthquake that struck the highlands of Dhamar in Yemen in December 13, 1982 caused around 400,000 people homeless [4].

The 1992 earthquake in Egpyt has caused death to at least 540 people, 6,500 injuries, and thousands of damaged buildings [5].

Earthquakes are generally defined and classified in terms of certain parameters such as magnitude, intensity, epicentral distance, and focal depth. Different types of earthquake hazards are generated when seismic events occur, but usually the most destructive type one is the severity of ground vibrations. This hazard can cause distortion, destruction, and collapse of natural and man made structures. Other secondary effects could presumably contribute to further destruction, if not given appropriate counter measures.

To minimize earthquake losses and mitigate their disastrous effects, a comprehensive study of earthquake nature, characteristics, and occurrences in spacetime is essential. One contributory aspect toward mitigation is the study of the basic relations among seismic parameters. In light of these relations, further studies in terms of correlation to other -physical entities can be undertaken to develop strategies for protection.

Because of regional peculiarities, a number of authors [6-18] have studied the basic relations among the seismic parameters. Due to the important applications of the parametric relations in the engineering field, other investigators [19-23] have correlated the seismic parameters to ground acceleration with the operation of appropriate types of instrumentation.

The attenuation relations are currently applied in the field of seismic hazard assessment, microzoning, seismic vulnerability and risk. Information obtained from these areas is useful in generating and preparing earthquake disaster preparedness plan in the national and regional level for the mitigation of earthquake losses. Since the present state of art in seismology cannot yet predict the time occurrence of seismic events, the best approach is a comprehensive preparation plan utilizing the scaling relations.

Thus, to contribute to the attainment of the objectives of earthquake mitigation, preliminary modeling of the scaling relations among the earthquake parameters is conducted for application in the study area (Fig. 1). The modeling approach is undertaken due to insufficient local parametric data that prevent direct determination of the scaling relations. Preliminarily, the modeled scaling relations can be applied in earthquake hazards estimation in the study region, within the limits of the utilized data. The estimates could provide supplemental support in assisting concerned agencies in making rational decisions for environmental protection.

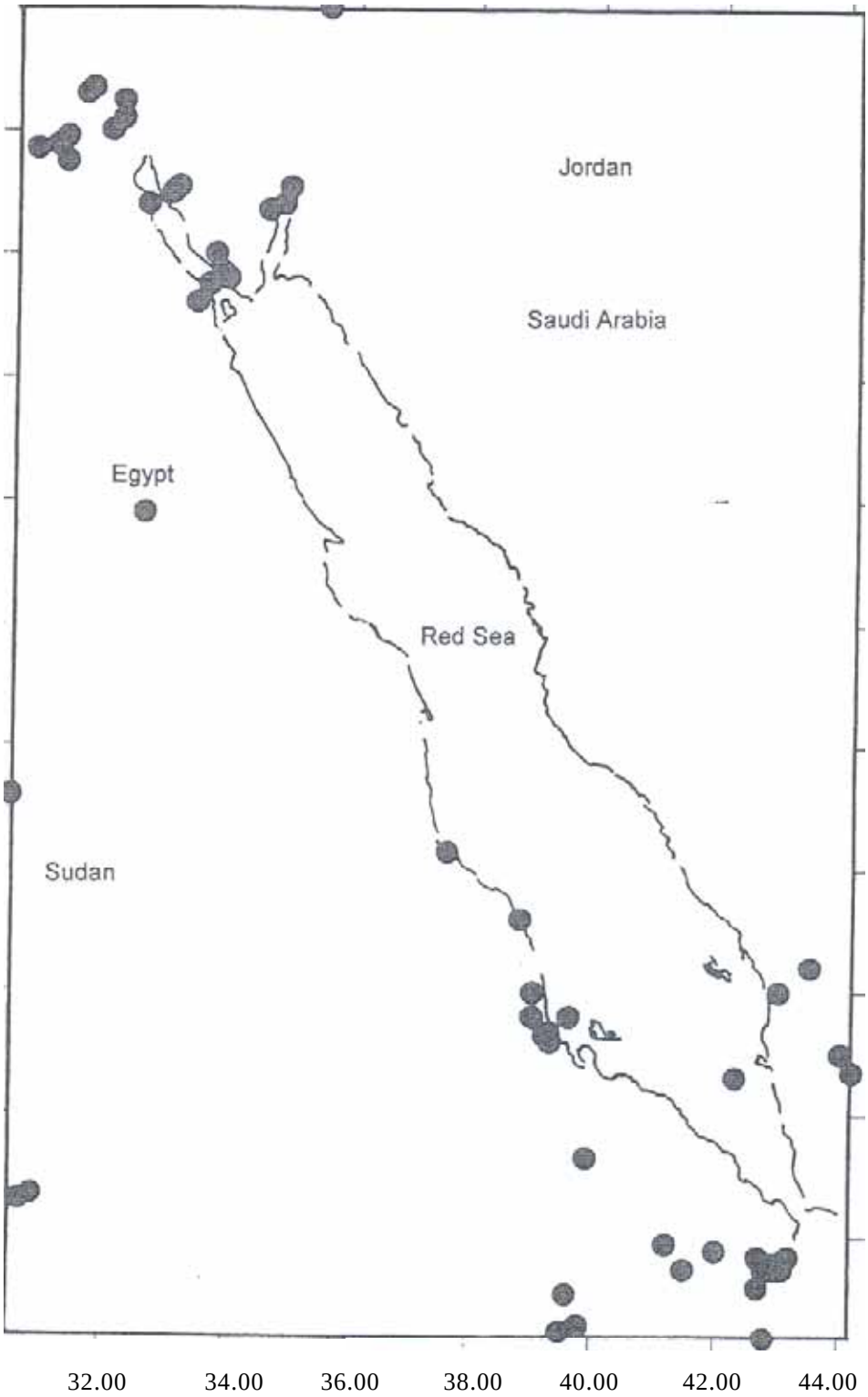

Fig. 1. Location map of study area. Solid circles represent earthquake events from the merged data base, irrespective of magnitude values.

Data and Materials

The earthquake parameters required for scaling relations are the surface-wave magnitude (Ms), body-wave magnitude (mb), intensity (I) in the Medvedev-Sponhueur-Karnik (MSK) Intensity Scale [24], epicentral (D) and hypocentral (r) distance, focal depth (h), and peak ground acceleration (PGA). A merged database is utilized in this study. The main data sources were the USGS preliminary determination of epicenters (PDE) (1965-1995), Ambraseys [19] compiled data for Saudi Arabia and adjacent areas, isoseismal maps drawn and prepared by Maamoun and El-Kashab [25], Maamoun *et al. [26],* Shehata *et al. [27],* Kebeasy *et al. [28],* Ibrahim [29], Ben Avraham and Tibor [30], Osman and Ghobarah [31]and PGA data from Amrat [32].

Re-analysis and slight modifications were conducted to some of the isoseismal maps to confonn to the general trends in the shapes and directivity of the isoseismal curves. To some extent, the minor modifications were done in consideration of some previously established international relations among the seismic parameters [6-18].

There were 23 observed focal depth from out of 50 seismic events taken from the merged database. Acceleration data were composed of 14 samples from 8 events. Allowing some percentage of non-inclusion of the data in the analysis due to inconsistencies, a relative insufficient number of these parameters exist. These constraints prompted this study to search for and apply alternative approaches in the determination of the scaling relations that lead to modeling processes.

No re-evaluation has been done to the other parametric data taken from the USGS PDE bulletins and Ambraseys [19], as it was assumed that comprehensive collection and compilation were conducted in the process of data acquisition. Moreover, flexibility in data handling and assigning parametric values were observed to be within allowable limits.

Procedure and Methodology

A. Intensity-distance relation

(a) The attenuation equation

The intensity attenuation equation with respect to distance can be derived from the concept of spherical propagation of energy in a homogeneous model. If E is the energy at the hypocenter, considered as a point at a depth (h), then the energy density at an

$$Er = Eexp(-cr)/(4(pi)r^2) \quad (1)$$

where $r^2= D^2+h^2$, and c is the seismic absorption coefficient. At the epicenter (r=h), the energy density is

$$Eo = Eexp(-ch)/(4(pi)h^2) \quad (2)$$

The ratio of the energy densities at the epicenter and epicentral distance D is

$$Eo/Er = (r/h)^2\exp(c(r-h)) \quad (3)$$

Taking decadic logarithm gives

$$\log(EolEr) = 21og(r/h) + c(r-h)\log e \quad (4)$$

From Weber-Fechner law [33,34, pp.459-461]

$$\log (Eo/Er) \_ (1\ /f)(Io-I) \quad (5)$$

where f is a constant, lo is the intensity at the epicenter, I is the intensity at D. Substitution of (5) in (4) gives

$$I = lo - k\log(r/h) - m(r-h) \quad (6)$$

where k=2f and m= cflog(e) are constants related to the attenuation rate and absorption coefficient respectively. When the depth of focus is not considered, (6) becomes

$$I = lo - k\log(D) - mD \quad (7)$$

(b) The initial data

Ten modified isoseismal maps in the MSK intensity scale description have been utilized in the study of intensity attenuation in the Red Sea region. Each isoseismal map is defined in terms of the earthquake event epicenter, magnitude, and focal depth, Table

Table 1. List of earthquake events with isoseismal map

Year	Lat(N)	Lon(E)	Mag(Ms)	Mag(Mb)	Depth(h)	Refer.
1847	29.7	30.8	5.8		15	[21]
1955	32.5	30	6.4	6.5	30	[21]
1966	12.6	30.7	5.6	5.1	22	[21]
1969	27.6	33.9	6.6	6.1	33	[20]
1981	23.8	32.6	5.5	5.1	10	[21]
1982	14.7	44.2	6.1	6	5	[22]
1987	30.5	32.2		5	24	[21]
1992	29.8	31.1	5.3	5.9	21	[23]
1993	28.7	34.5	5.8	5.9	10	[24]
1995	28.8	34.8	7.3	62	10	[25]

On each isoseismal map (Figs. 2-3), diagonal lines in many arbitrary directions were drawn from the epicenter to the isoseismal curves. The epicentral distances associated to each of the iso-intensity curves are the line segments of the diagonals drawn from the epicenter intersecting the respective isoseismal curves. The line

segments were measured and converted to distance (km) from the given scale in each map respectively, and the corresponding mean epicentral distance for each isoline is calculated. From the mean epicentral distances, the respective mean hypocentral distances were computed with the corresponding depths of foci. The respective intensities were plotted against the corresponding mean hypocentral and epicentral distances separately as shown in Figs. 4-5. It is presumed that in taking the average values of the hypocentral and epicentral distances lead to homogeneous modeling of the actual conditions portrayed in each isoseismal map.

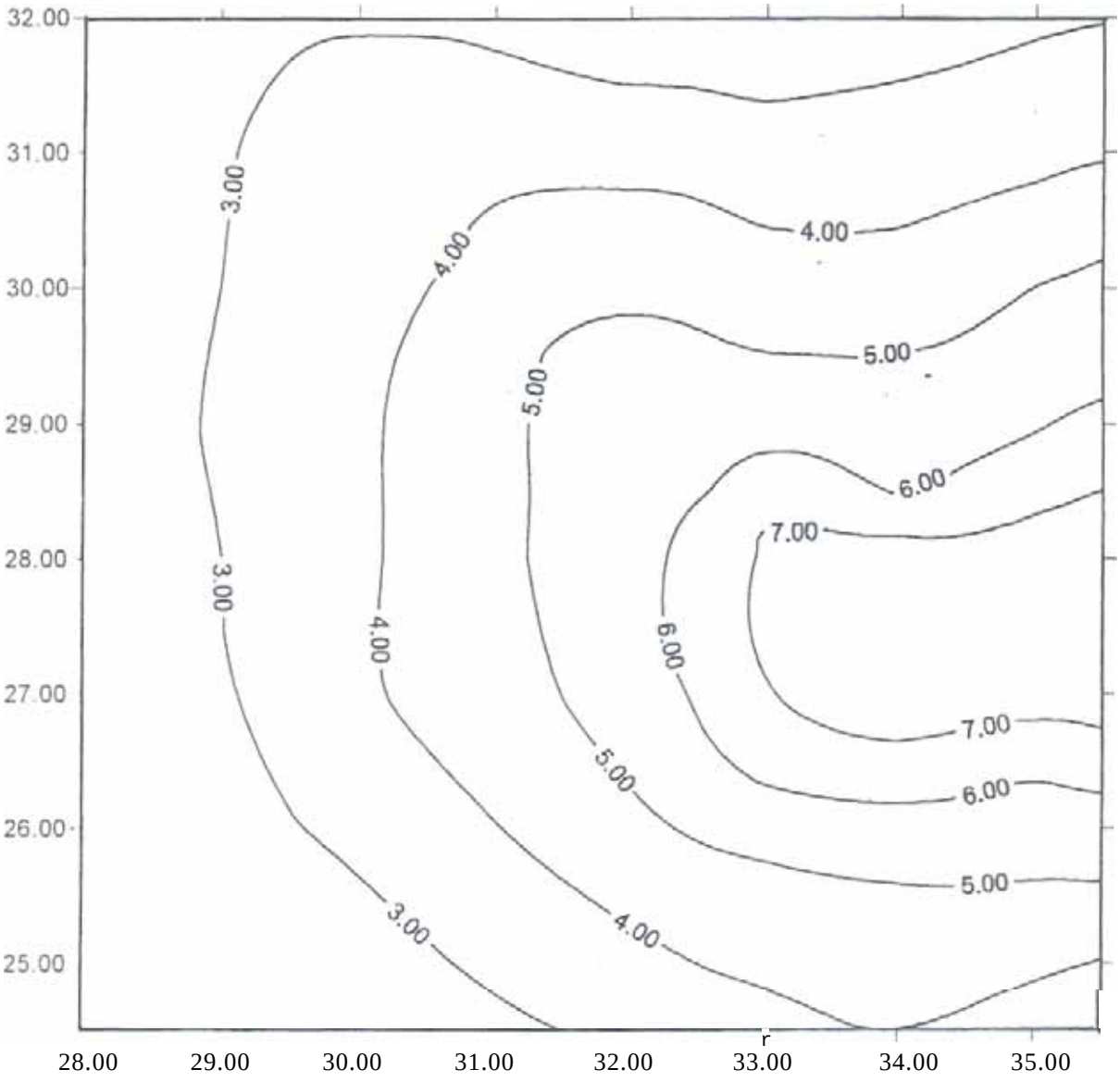

Fig. 2. Alodified computerized isoseismal map of 1Iarch 31, 1)6) earthquake in the northern Red Sea. Epicenter: 27.7N; 3=1E. Reference: ;Maamoun and El-tiashab (1978) isoseismal lines are based on MSK intensity scale.

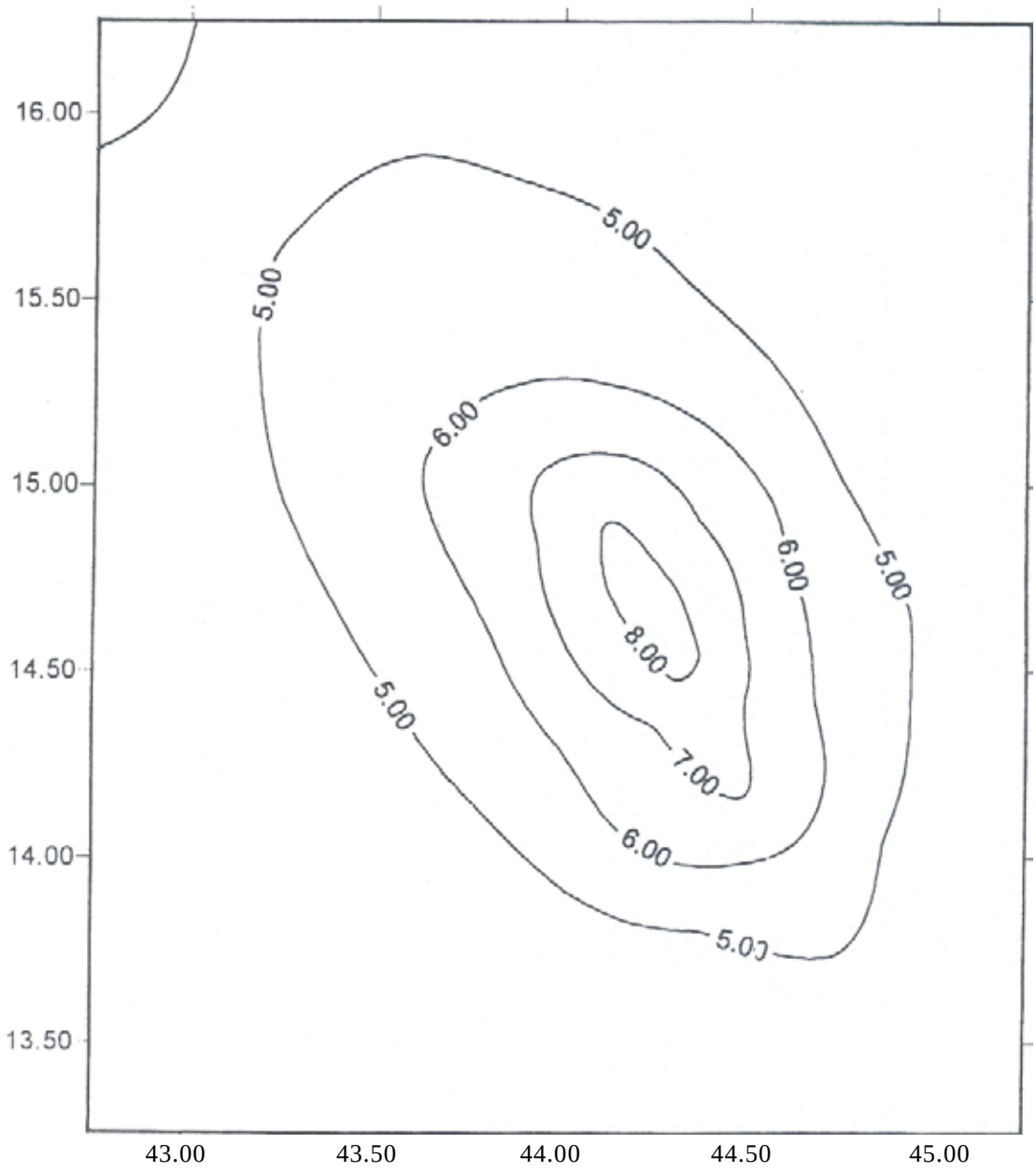

Fig. 3. Computerized isoseismal map of December 13, 1982 earthquake in Dhamar, Yemen. Macroseismic epicenter 14.68 N; 44.24 E. Reference Shehata et *nL* (1983). Isoseismal lines are based on 16'ISK intensity sale.

(c) Modeling the intensity attenuation relation

Each plot of the mean hypocentral and epicentral distances against corresponding intensity (Figs. 4-5) was fitted by (6) and (7) respectively by means of regression analysis.

There were 10 set of lo, k, and m values for (6) and another 10 for (7) obtained by this method of fitting as shown in Table 2. In Table 2, there were two ranges of values for the seismic absorption coefficient. They are classified as low and high anelastic attenuation coefficients. In practice, it is tedious and cumbersome to use many

العلاقات القياسية للمعاملات الزلزالية في منطقة البحر الأحمر

بنيتو بونزا لان و عبدالله العمري

مركز الدراسات الزلزالية، جامعة الملك سعود، الرياض، المملكة العربية السعودية

(قدم للنشر في ١٤٢٢/٧/١٩هـ؛ وقبل للنشر في ١٤٢٣/١/٢٦هـ)

ملخص البحث. العلاقات القياسية لتخامد الشدة الزلزالية والتعجيل الأرضي الأقصى بالنسبة لبعدها عن مركز الزلزال السطحي والمسافة البؤرية والقدر الزلزالي للموجات السطحية والباطنية والعمق البؤري تم تطويرها لتطبيقها في منطقة البحر الأحمر.

علاقات التخامد تم تحديدها من النمذجة المتجانسة للخرائط الزلزالية المعدّلة للأحداث الزلزالية من مناطق مختلفة ومن معلومات التعجيل الأرضي الأقصى ومن تحويل الشدّة الزلزالية إلى القدر الزلزالي مع العمق البؤري.

عمومًا المعادلات القياسية المشتقّة في هذه الدراسة يعبّر عنها بالآتي:

I = aiMi-bi log(D+Di) - ciD-di log(h)+ei
I = aiMi-bi log(r/h)-ci(r-h)-di log(h)+ei
Log(PGA)=aiMi-bi log(D+Di)-ciD-di log(h)+ei
Log(PGA)=aiMi-bi log(r/h)-ci(r-h)-di log(h)+ei

حيث إن المعاملات ai، bi، ci، و di تمثل على التوالي القدر الزلزالي، المسافة، معاملات التخامد اللامرن والعمق البؤري. أما Di فهي تمثل نصف القطر التقريبي للمطقة الزلزالية Meizoseismal المناظرة لنوع معامل التعتيم و ei ثابت مختلف.

نتيجة هذه الدراسة سوف تساعد على تطوير الطرق الضرورية والأساسية لتقدير الحركة الأرضية في منطقة البحر الأحمر. وكمصدر إضافي للمعادلات في تقدير الخطر الزلزالي فإن هذه العلاقات القياسية سوف تساعد في صياغة قرارات استراتيجيات حماية البيئة.

equations. Hence, reducing the initial findings for less number of relations was envisioned to be developed for the different types of attenuation coefficients. The concept in modeling approach is to find a new value for k and m for each of the two types from the different values of k and m belonging to each type, that are presumably representative for any value of Io and appropriate for application in the study area. To start with, equation (6) is differentiated with respect to hypocentral distance

$$dI/dr = -k\log(e)/r - m \quad (8)$$

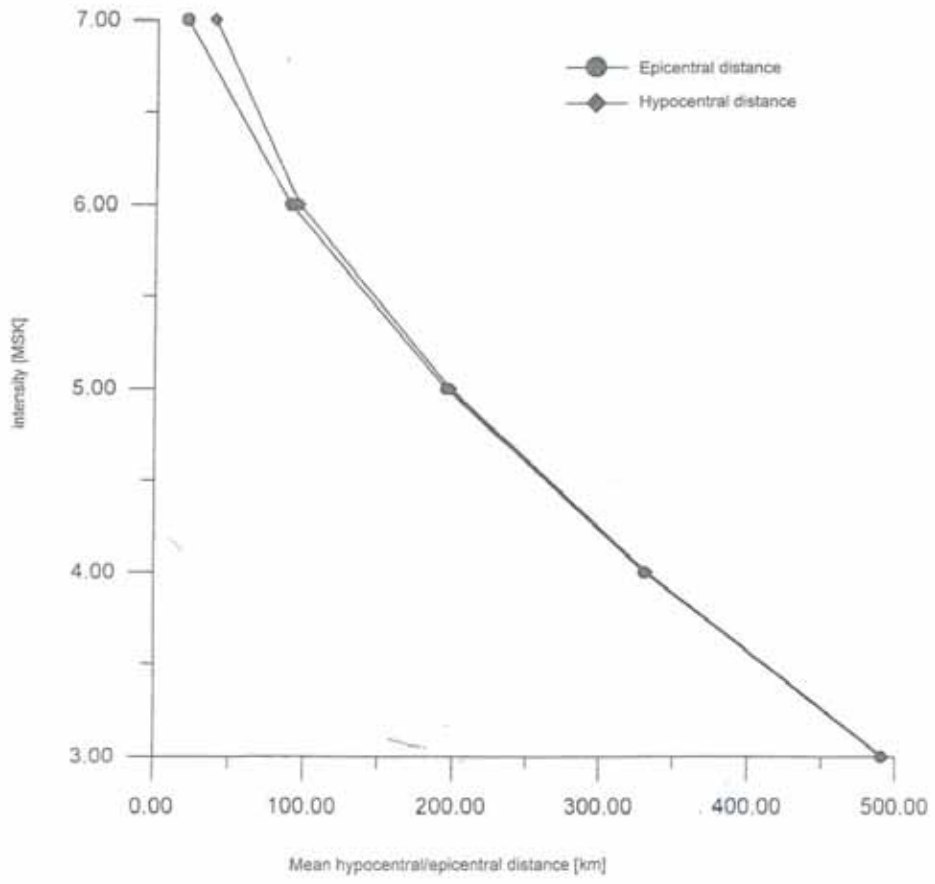

Fig. 4. Intensity mean distance graph of March 31, 1969 earthquake in Egypt.

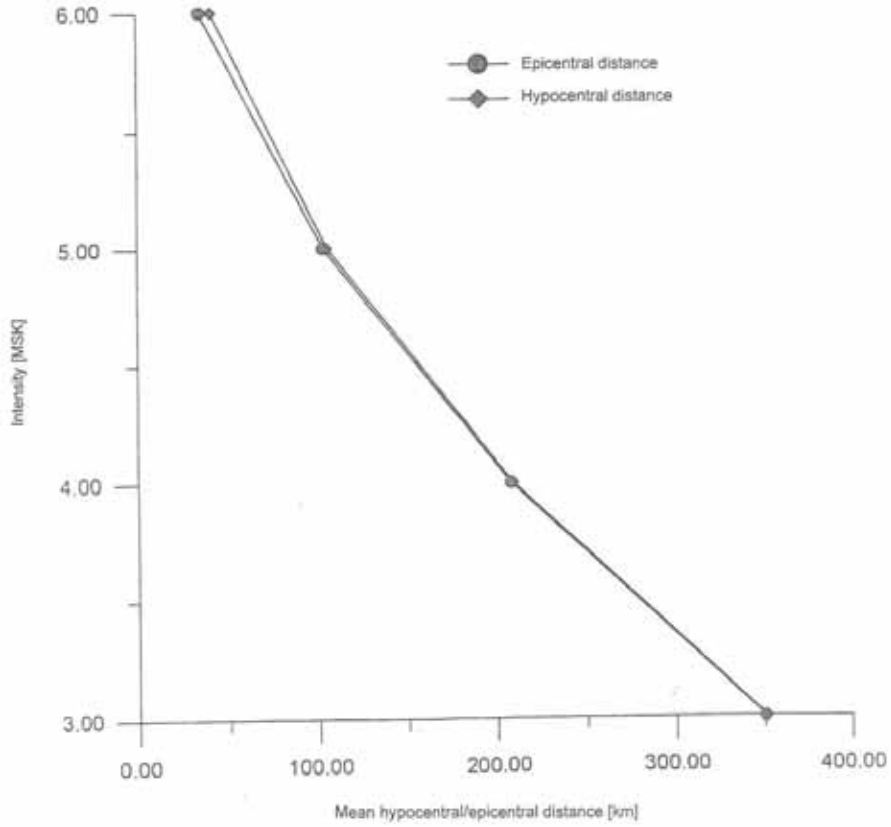

Fig. 5. Intensity-mean distance graph of October 12m 1992 earchquake in Egypt.

Table 2. Regressed intensity attenuation relations

	Epicentral distance			Hypocentral distance		
Year	Io	k	m	Io	k	m
1847	8.84	1.654	0.0048	7.99	1.218	0.0059
1955	8.8	1.638	0.0056	6.49	2.293	0.0046
1966	9.58	1.288	0.0213	7.92	1.16	0.212
1969	8.47	1.035	0.0055	7.15	1.87	0.0042
1981	8.8	1.312	0.0051	7.56	1.457	0.0047
1982	10.69	2.202	0.0183	9.8	1.702	0.0207
1987	8.93	1.29	0.0199	7.04	1.276	0.0197
1992	8.45	1.472	0.0049	6.58	1.815	0.0043
1993	9.85	2.797	0.011	8.12	1.784	0.0162
1995	10.54	1.635	0.005	9.95	1.382	0.0053

The value of the slope (dI/dr) can be estimated at arbitrary values of D (km), since k and m are previously known from the regressed equations, and h is given (Tables 1 and 2). The slopes at every increment of 50 km, starting from 50 km epicentral distance up to 500 km were calculated. Calculation is done for each corresponding values of k and m. The average value of the slopes at corresponding average hypocentral distances were computed, and the respective values were plotted as shown in Figs. 6-7. Each point in the plot corresponds to (-dI/dr, r), so that the plots are graphs of differential equations. It can be seen that the graphs of the data points resemble generally a hyperbolic equation

$$Y = q/r + g \tag{9}$$

where q and g are the modified constants to be determined by regression techniques, and Y= -dI/dr. After determining the values of the constant q and g, the regressed equation is integrated to obtain the equation of the integral curve (I, r) [35,pp.6-10]. This method of treatment reverts back to (6), where Io is now an arbitrary constant. The empirical relation that was obtained in Fig. 6 for the (I, r) equation for the low attenuation coefficient after integration was

$$I = Io - 1.85\text{Log}(r/h) - 0.0047(r-h) \tag{10}$$

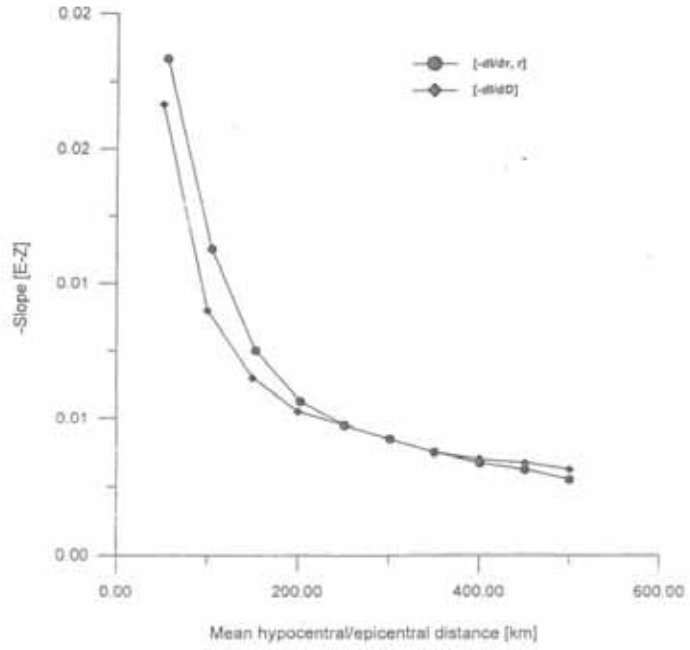

Fig. 6. Stop-mean distance graph [low rate].

Applying the same method of approach and treatment to equation (7), the intensity and epicentral distance (I, D) empirical relation for the low attenuation coefficient can be determined (Fig. 6). This was found to be

$$I = Io - 1.37\text{Log}(D) - 0.0053\,D \tag{11}$$

However, the real estimate on the true value of Io is given in (10), while the apparent value is from (11). In Table 2, the apparent values can be reduced to the true values by adding a constant epicentral distance Do to D, since Io in (10) is estimated when D is zero. From the difference of the apparent and true values of Io, the average value of Do was found to be 13 km. Hence, (11) becomes

$$I = Io - 1.37\log(D+13) - 0.0053D \tag{12}$$

where Io is the apparent value. In (12), the value of Do can be considered as the approximate radius of perceptibility of the meizoseismal area.

In applying the same method and treatment to the high attenuation coefficient (Fig. 7), the following (I, r) and (I, D) relations were obtained respectively:

$$I = Io - 1.8\log(r/h) - 0.018(r-h) \tag{13}$$

and

$$I = Io - 2.2\log(D+6) - 0.015D \tag{14}$$

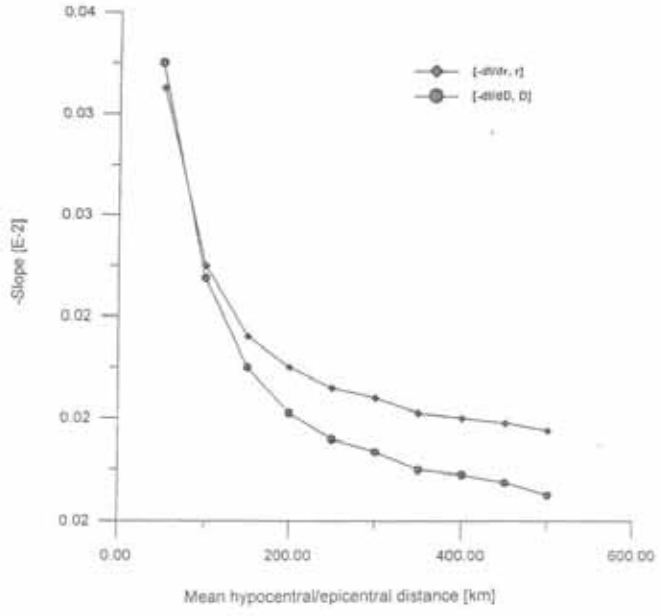

Fig. 7. Slope-mean distance graph [high rate].

For discussion purposes, (10) and (12) are considered as low rate attenuation in terms of the parameter r and D, while (13) and (14) as high rate attenuation in r and D respectively.

The assessment of Io is not immediately available, and sometimes its evaluation encounters time delay and physical constraints, especially if the epicenter is inaccessible and devoid of the factors from which intensity is estimated, such as the effects to population and infrastructures. In such cases, the practical application of (10) or (12), and (13) or (14) for immediate assessment of earthquake danger in affected places becomes ineffective. Perhaps, these conditions prompted the authors [14,15,20,23] to correlate the instrumental magnitude to Io. The magnitude is a measured quantity from instrumental recordings, and handily available as inference, compared to intensity which is a subjective parameter.

B. Magnitude – epicentral intensity relation

Statistically, the data in Table 2 are insufficient to determine the representative empirical relation between magnitude and epicentral intensity. The initial data were augmented from the merged database. A total of 50 Ms and 29 Mb data with their corresponding Io were plotted in Figs. 8-9. The relation established by the investigators [14,15,20,23], where a and b are constants and the subscript i indicating the type of magnitude was fitted. The obtained values for the coefficient (a) for Ms and Mb were too low, (0.29) and (0.2) respectively, compared to the international value range which is from 0.4 – 0.7. One probable cause of the low values is the wide scattering of data points due to under or over estimation of the epicentral intensities. This notion was slightly considered, since the data points seemed to form into different and distinct groupings. The other factor for the low value could be due to the influence of geology, but possibly tolerable due to consideration of a single geological unit for most parts of the region. Assuming these factors have minimal contributions to the low value of the coefficient a, then another alternative approach and data treatment have been undertaken.

$$Mi = aiIo + bi \qquad (15)$$

Scatter of the data points into different clusters is observable for both Ms and mb plots, but the clusters in each plot seemed to be oriented linearly at some inclination from the horizontal. Since the data points are conglomeration of different values of magnitude, epicentral intensity, and focal depth, then different clusters (A,B,C,D,E,F) bounded by solid lines as shown in Figs. 8 -9, were treated and fitted with equation (15) separately. A probable logical explanation for the group clustering is the tendency of the data points to stick with the cluster of the same depth value range, since intensity is influenced by the focal depth. Following this line of argument, the obtained regressed relations were

$$\text{Cluster A}: \quad Ms = 0.65Io + 2..2 \qquad (16\,a)$$

$$\text{Cluster B}: \quad Ms = 0.65Io + 1.36 \qquad (16\,b)$$

Cluster C :	Ms = 0.66Io + 0.82	(16 c)
Cluster D :	mb = 0.55Io + 2.8	(16d)
Cluster E :	mb = 0.54Io + 2.13	(16e)
Cluster F :	mb = 0.53 + 1.25	(16f)

In (16a, 16b, 16c), the coefficients of Io for the Ms-Io relation have almost the same values, while the constants differ. Likewise, the same situation is also observed in (16d, 16e, 16f) for the mb-Io relation. The above results follow from the assumption that each cluster belongs to different depth value range. Quantitatively, it requires a larger magnitude value at deeper focal depth to be felt at the same level of intensity at the epicenter with a smaller magnitude earthquake situated at a shallower focal depth.

Due to insufficiency of numerical values for the focal depth in each cluster, the results cannot be confirmed for correctness of the constants. Nonetheless, the influence of the focal depth to assessment of earthquake hazards is essential and important. To establish a preliminary basis for the empirical relation between focal depth, magnitude, and epicentral intensity, a modeling scheme was undertaken.

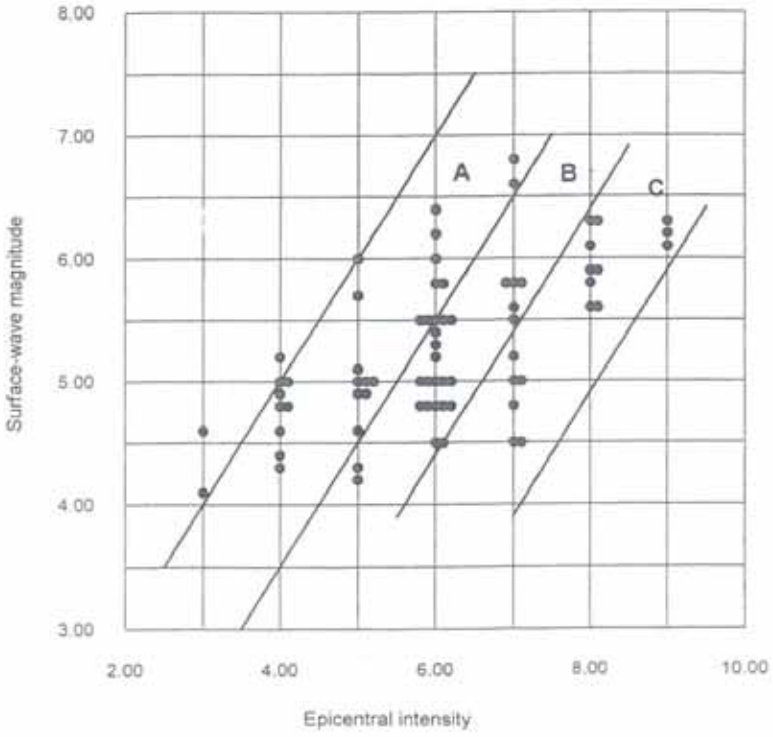

Fig. 8. Surface-wave magnitude-epicentral intensity graph. Some solid circles are displaced along the intensity axis to show the number of data belonging to these particular points.

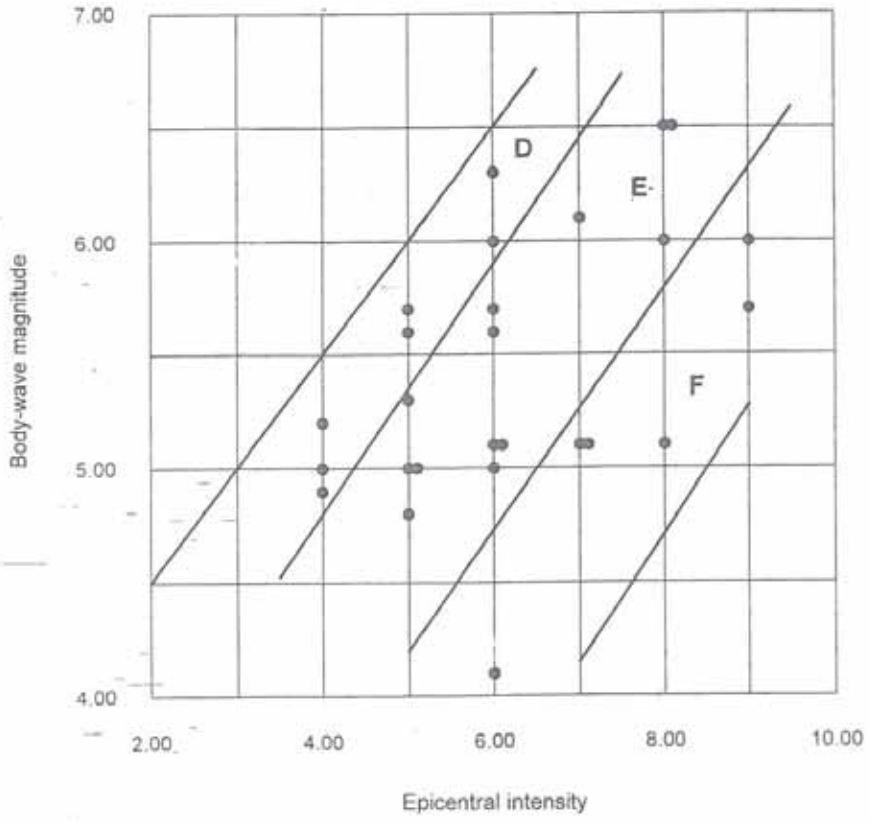

Fig. 9. Body-wave magnitude-epicientral intensity graph. Soild circles are displaced along the intensity axis to show number of data belonging to these particular points.

C. Modeling magnitude-intensity-depth relation

In relations (16a, 16b, 16c), the coefficient (a) was taken as 0.65 due to median value consideration and number of data events in each cluster. In the same consideration, the value 0.54 was selected for the coefficient in the mb-Io relation. Using these values, the difference (Ms–0.65Io) and (mb-0.54Io) for each of the utilized earthquake events was estimated. The difference values for the Ms-Io and mb-Io relations were arranged separately in ascending order of magnitude. The shallowest observed focal depth from the database is 5 km, while the deepest is 57 km. Using this range of focal depth, the smallest and largest difference values for (Ms-0.65Io) and (mb-0.54Io) were made to correspond to 5 km and 57 km respectively. This arrangement was selected since the epicentral intensity for shallow focus earthquakes is relatively of higher degree than that of an event at deeper focus. This situation makes the difference value between magnitude and epicentral intensity in the relation a small quantity for shallow events.

The magnitude-intensity-depth relation is linear in the decadic logarithm of the depth (h). This is given as

$$Mi = aiIo + filog(h) + di \quad (17)$$

which was commonly used and established in different studies [14,15,16,18], where f and d are constants to be known, with the subscript i indicating the type of magnitude considered. From the preliminary assigned focal depths, the distribution of corresponding depth for the other difference values were determined by interpolation procedure subject to the linearity of (17). Using regression analysis, the approximate empirical relations were found to be

$$Ms = 0.65Io + 2.2log(h) - 1.3 \quad (18)$$

and

$$mb = 0.54Io + 2.3log(h) - 0.95 \quad (19)$$

D. Interrelations from scaling relations

Developing interrelations from the scaling relations is necessary in the aspects of application. The interrelations are the results of simplifying and expressing the scaling relations to parameters that are handily available and quantifiable.

Eliminating Io in (10), (12), (18), and (19), gave the resulting equations for the low rate:

$$I=1.54Ms-1.37log(D+13)-0.0053D-3.4log(h)+2 \quad (20a)$$
$$I=1.85mb-1.37log(D+13)-0.0053D-4.3log(h)+1.8 \quad (20b)$$
$$I=1.54Ms-1.85log(r/h)-0.0047(r-h)-3.4log(h)+2 \quad (20c)$$
$$I=1.85mb-1.85log(r/h)-0.0047(r-h)-4.3log(h)+1.8 \quad (20d)$$

Elimination of Io in (13), (14), (18), and (19) yield the following expressions for the high rate:

$$I=1.54Ms-2.2log(D+6)-0.015D-3.4log(h)+2 \quad (21a)$$
$$I=1.85mb-2.2log(D+6)-0.015D-4.3log(h)+1.8 \quad (21b)$$
$$I=1.54Ms-1.8log(r/h)-0.018(r-h)-3.4log(h)+2 \quad (21c)$$
$$I=1.85mb-1.8log(r/h)-0.018(r-h)-4.3log(h)+1.8 \quad (21d)$$

However, intensity as a subjective and dimensionless entity is not acceptable in engineering fields. For useful applications, studies were made regarding the relation of intensity and ground acceleration. The results obtained by Trifunac and Brady [23], Bath [21], and the relation between intensity and ground acceleration deduced from the given acceleration ranges in the MSK scale [24,33] are as follows respectively:

$$log(Ah) = 0.3I - 0.014 \quad (22a)$$

$$\log(A) = 0.3I - 1.5 \quad (22b)$$
$$\log(Amax) = 0.3I - 0.11 \quad (22c)$$

where Ah, A, and Amax in gals are the horizontal ground acceleration, ground acceleration, and maximum value of acceleration in each intensity grade respectively. It is shown in the 3 relations that the coefficients of I are of the same value, differing only with the constant term. Substitution of (22c) as preference in (20a) up to (21d) gives the following equations for the low rate:

$$\log(Amax)=0.46Ms-0.4\log(D+13)-0.0016D-\log(h)+0.57+d1 \quad (23a)$$
$$\log(Amax)=0.46Ms-0.56\log(r/h)-0.0014(r-h)-\log(h)+0.57+d2 \quad (23b)$$
$$\log(Amax)=0.56mb-0.4\log(D+13)-0.0016D-1.28\log(h)+0.5+d3 \quad (23c)$$
$$\log(Amax)= 0.56mb-0.56\log(r/h)-0.0014(r-h)-1.28\log(h)+0.5+d4 \quad (22d)$$

For the high rate:

$$\log(Amax)=0.46Ms-0.65\log(D+6)-0.0046D-\log(h)+0.57+d5 \quad (24a)$$
$$\log(Amax)=0.46Ms-0.55\log(r/h)-0.0054(r-h)-\log(h)+0.57+d6 \quad (24b)$$
$$\log(Amax)=0.56mb-0.65\log(D+6)-0.0046(D+6) -1.28\log(h)+0.5+d7 \quad (24c)$$
$$\log(Amax)=0.56mb-0.55\log(r/h)-0.0054(r-h)-1.28\log(h)+0.5+d8 \quad (24d)$$

where the di with i from 1 to 8 are considered constants to be adjusted after testing the validity of the attenuation equations with the observed Gulf of Aqaba PGA data from Amrat [32]. The outcomes in applying this procedure for the low rate were:

$$\log(PGA)=0.46Ms-0.4\log(D+13)-0.0016D-\log(h)+0.78 \quad (25a)$$
$$\log(PGA)=0.46Ms-0.56\log(r/h)-0.0014(r-h)-\log(h)+0.33 \quad (25b)$$
$$\log(PGA)=0.56mb-0.4\log(D+13)-0.0016D-1.28\log(h)+0.73 \quad (25c)$$
$$\log(PGA)=0.56mb-0.56\log(r/h)-0.0014(r-h)-1.28\log(h)+0.31 \quad (25d)$$

For the high rate:

$$\log(PGA)=0.46Ms-0.65\log(D+6)-0.0045D-\log(h)+1.43 \quad (26a)$$
$$\log(PGA)=0.46Ms-0.55\log(r/h)-0.0054(r-h)-\log(h)+0.53 \quad (26b)$$
$$\log(PGA)=0.56mb-0.65\log(D+6)-0.0045D-1.28\log(h)+1.39 \quad (26c)$$
$$\log(PGA)=0.56mb-0.54\log(r/h)-0.0054(r-h)-1.28\log(h)+0.54 \quad (26d)$$

Provided, the assumptions and modeling processes, sufficiency and accuracy of the data are valid and acceptable, equations (20), (21), (25), and (26) are locally applicable in the estimation of ground motion as a first approximation, in areas that conform to the corresponding attenuation rate in the region.

Discussion of Results

There are eight scaling relations (20a - 20d and 23a - 23d) for intensity and acceleration attenuation in terms of epicentral and hypocentral distance and magnitude Ms and mb for the low rate. Likewise, there are also eight scaling relations (21a - 21d and 24a - 24d) with the same parameters for the high rate. The purpose of all these relations is mainly due to the needs and requirements in applicability. Usually, local seismographic networks do not cater and possess the appropriate type of instrumentation for surface-wave magnitude determination, except for special purposes. The main interest of local networks is the detection and determination of the seismic parameters of local and near events. It follows that the development of magnitude formulas are presumably locally calibrated using mb values as standard, for the establishment of an independent and immediate reactions in times of earthquake emergencies. Ms values are mostly determined routinely by international agencies for major and large-scale events, and infrequently for strong and moderate events. Ms values are preferable because they reflect the total seismic energy, but the restraining factors and requirements in their determination are deterrent processes. The same constraint also arises for the focal depth when the resolution is poor. This leads to uncertainties in the results of computations, such that it may be appropriate to use the parameter D instead of r in the scaling relations.

There were two types of anelastic attenuation coefficients found from the initial data of the modified isoseismal maps. The low coefficient is associated with earthquake events originating from the interior portion of the shelf and massif areas in the Red Sea region. For example the 1969, 1981, and 1992 earthquakes in the territory of Egypt belong to this coefficient. The 1982 Yemen earthquake, the 1987 Egypt earthquake, and the 1993 Gulf of Aqaba earthquake belong to the high coefficient. These earthquake events are located in the Yellow Trap Series volcanic in northern Yemen, extension of the main fold axis of the mountainous region from Lebanon, and in the Aragonese Deep which is one of the depressions at step zones in the Gulf of Aqaba respectively. It seems that rift systems associated with geophysical anomalies and folding mechanisms are associated to the high coefficient. Associated to the low coefficient are continental areas that are efficient in propagating ground vibrations. Such observations prompted separate consideration for the anelastic attenuation coefficients, and constrained the selective application of attenuation equations to appropriate areas in the Red Sea region for better results.

In the Mi-Io-h relation, the focal depth of an earthquake is a vital factor that contributes to the degree of ground shaking in the epicentral area. Shallow seismic events are usually destructive even for moderate earthquakes. The coefficients obtained for log(h) in the Mi-Io-h relation were very close to that found by Shebalin [18].

Values obtained from the present modeled attenuation equations can be considered as a first approximation. The relations were the outcomes from assumptions and homogeneous modeling. Modified and accurate results can be taken from dense

networks of the appropriate type of seismic instrumentation that may not be feasible at present. In the meantime, the present findings are suitable as supplements or alternatives to related formulas used in specified areas in the region within the limits of the utilized data.

It was noted that in testing the acceleration attenuation equations in terms of the PGA values from Amrat [32] data, the high rate equation (26c) gave better correlation to the observed values. The percentage error ranges were approximately 6%- 13% for 8 samples, and 23% for 2 samples from 10 total samples. For the (26a) relation for the high rate, the percentage error ranges were approximately 4%-12% for 4 samples, and 22%-32% for 3 samples from 7 total samples. The percentage error range for the low rate (25c) relation is approximately 2%-17% for 7 samples, and 23%-30% for 3 samples from 10 total samples. The high rate attenuation equations (26a-26d) gave better correlation to the observed values is an indication of the appropriateness of the relations due to conformity with the source type of earthquake occurrences in the Gulf of Aqaba.

The other relations (25a-25d) gave wide range of percentage error from approximately 1%-62%. The wide range of error in relations (25a-25d) does not reflect inaccuracy, but the absence of the appropriate observed PGA values for the test. The 1% error is an indication of validity for these relations, which might be connected to the source path of the generated seismic waves and the geographical location of source and sites. The high percentage error in all the acceleration attenuation equations could presumably be related to the discrepancies regarding epicenters in the USGS seismic bulletin and Amrat [32] data for the earthquake events in Aug.2, 1993, Sept. 16, 1994, and Nov. 22, 1995. Since the attenuation equations are partly dependent on distance, the discrepancies could affect the outcomes of the test. However, this supposition cannot be verified because the coordinates of the sites from which the observed PGA values were recorded were not mentioned. Other affecting factor is the focal depth. At relatively farther distances, the value of r approaches that of D for shallow focus. From the 8 events that were used, 7 events have focal depth of 10 km. given in the USGS bulletin. At these conditions, the estimates from the attenuation equation dependent on D gave better results.

Comparison of equations (23) and (25) shows that the additive constant (di) gave positive and negative values for the relations with the D and r parameters respectively. On the other hand, the additive constants in the high rate with the r parameter gave negative and positive values in (26b) and (26d) respectively. The explanation for these observations depends upon the value assumed by r and D. The parameter r is longer in length than D, so that the values obtained with the term r are approximately larger to incur negative or smaller di values for adjustment.

Conclusion

The developed scaling relations of earthquake parameters are preferable in application due to regional peculiarities in the geologic structures, and utilization of domestic seismic data that satisfy the requirements of national needs and development. Initial test of the preliminary developed acceleration attenuation equations from observed PGA values had shown certain degree of accuracy, despite inadequacy of data appropriateness and possible data discrepancies. This may indicate that the assumptions and modeling approaches are presumably valid and acceptable. The acceptability and validity also imply for the intensity attenuation equations due to correlation of the two parameters. Hence, the developed attenuation equations could be sources of ground motion estimation formulas for first approximate values in the study area, subject to further improvement from appropriate dense seismic instrumentation network.

Acknowledgement. We wish to express our gratitude to those who have contributed to the preparation of this manuscript.

References

[1] United Nations Conference on Human Settlements. *Conference Background Paper*, A/Conf. 70/8/7, 24 Feb. 1976, Vancouver, Canada.
[2] Shirong, Mei. *The Tangshan Earthquake of 1976*. Beijing, China: Seismology Publ. House, 1982,
[3] Lomnit, C. "Some Observation of Gravity Waves in the 1960 Chile Earthquake". *Bull. Seismo. Soc. Am.*, 60 (1970b), 669-670
[4] Erdik, M. *22 December 1991 Yemen Earthquake. Soil Dyn. Earthq. Eng'g*, 11 (1992), 327-334
[5] El-Sayed, A., Arvidsson, R. and Kulhanek, O. "The 1992 Cairo Earthquake". *Comprehensive Summaries of Uppsala Dissertations*. Sweden: Fac. Sci. Tech., Univ. Upssala, 262 (1997).
[6] Anderson, J.G. "On the Attenuation of Modified Mercalli Intensity with Distance the United States". *Bull. Seism. Soc. Am.*, 68 (1978), 1147-1179
[7] Chandra, U. "Attenuation Intensities in the United States". *Bull. Seism. Soc. Am.*, 69 (1979], 2003-2024
[8] Everden, J.F. "Seismic Intensities 'Size' of Earthquakes and Related Parameters". *Bull. Seism. Soc. Am.*, 65 (1975), 1287-1313
[9] Gupta, I.N. "Attenuation Intensities Based on Isoseismal of Earthquakes in Central United States". *Earthq. Notes*, 47 (1976), 13-20
[10] Gutenberg, B. and Richter, C.F. "Earthquake Magnitude, Intensity, Energy and Acceleration". *Bull. Seism. Soc. Am.*, 32 (1942), 163
[11] Gutenerg, B. and Richter, C.F. "Earthquake Magnitude, Intensity, Energy and Acceleration". *Bull. Seism. Soc. Am.*, 46 (1956), 105
[12] Howell, B.F. and Schulltz, T.R. "Attenuation of Modified Mercalli Intensity with Distance from the Epicenter". *Bull. Seism. Soc.Am.*, 65 (1975), 651-665
[13] Kaila, K.L. and Sarkar, D. "Earthquake Intensity Pattern in India". *Proc. Symp. Analysis of Seismicity and on Seismic Risk*, 173-191, *Liblice*, Chzechoslavakia. Oct. 17-22 (1977)
[14] Karnik, V. "Magnitude-intensity Relations for European and Mediterranean Seismic Regions". *Studia Geophy. et Geod.*, Praha 9 (1965). 23b
[15] Karnik, V. "Intensity-distance Relation for European Earthquakes and Its Application". Studia Geophy. et Geod., 9 (1965), 341.
[16] Kawasumi, H. "Intensity and Magnitude of Shallow Earthquakes". *Publ. BCIS, Tr. Sc.*, 19 (1956), 99.
[17] Nutli, O.W. "Seismic Wave Attenuation and Magnitude Relations for Eastern North America". *Jour. Geophy. Res.*, 78 (1973), 876-885
[18] Shebalin, N.V. "On the Relation Among Energy, Intensity and Focal Depth of Earthquakes". *Izvestiya. Akad. Nauk USSR. Ser. Geofiz.*, (1955), 377

[19] Ambraseys, N.N. "The Seismicity of Saudi Arabia and Adjacent Areas". *ESEE Research Report. Eng'g Seism. Earthq. Eng'g.* No. 88/11, 218pgs., London: Imperial College, 1988.
[20] Ambraseys, N.N. "The Correlation of Intensity with Ground Motions". *Proc. 14th Assem. Europ. Seism.Comms.*, 1 (1974), 335-341, Italy.
[21] Bath, M. "Earthquake Energy and Magnitude". In: *Physics and Chemistry of the Earth.* Pergamon Press, 1966.
[22] Campbell, K.W. "Near Source Attenuation of Peak Horizontal Acceleration". *Bull. Seism. Soc. Am.*, 71 (1981), 2039-2070
[23] Trifunac, M.D. and Brady, A.G. "On the Correlation of Seismic Intensity Scales with the Peaks of Recorded Strong Ground Motion". *Bull. Seism. Soc. Am.*, 65 (1965), 139-162
[24] Medvedev, S.V., Sponheuer, W. and Karnik, V. "Intensity Scale of Earthquakes". *IUGG, IASPEI, Berlin H*, 1964, 77.72
[25] Maamoun, M. and El-Kashab, H.A. "Seismic Studies of Shadwan Red Sea Earthquake". *Bull. Helwan Inst. Astr. Geophy.*, 170 (1978).
[26] Maamoun, M., Megahed, A. and Allam, A. "Seismicity of Egypt". *Bull. Helwan Inst. Astr. Geophy., Ser. B* (1984), 109-160
[27] Shehata, W.M., Kazi, A., Zakir, F.A., Allam, A.M. and Sabtan, A.A. "Preliminary Investigations on Dhamar Earthquake, North Yemen, of December 13, 1982". *Bull. King Abdulaziz Univ.*, (1983), 23-52
[28] Kebeasy R., Maamoun, M., Albert, R. and Megahed, A. "Earthquake Activity and Earthquake Risk Around Alexandria". *Bull. LIEGE*, 19 (1982), 93-113
[29] Ibrahim, I. "Seismicity and Seismic Hazard in Egypt: The Earthquake of Dashour of 12,10,1992, *XXII' Gen. Assembly*, (1994) Sept. 19-24, Athens, Greece.
[30] Ben Avraham, Z. and Tibor, G. "The Northern Edge of of the Gulf of Elat". Tectonophysics, 226 (1993), 319-331.
[31] Osman, A. and Ghobarah, A. "The Aqaba Earthquake of November 22, 1995". *EERI Special Report*, 1996.
[32] Amrat, A.F. "Empirical Relations Characterizing Earthquake Ground Motion Attenuation in Jordan". *JSO, NRA, Bull.*, 28 (1996), 37-45.
[33] Zatopek, A. "Lecture Notes 9". *Inter. Inst. Seism. Earthq. Eng'g*, Tokyo: Japan (1969).
[34] Serway, R. *Physics for Scientists and Engineers*, Updated Version, 3rd ed., Saunders Golden Sunburst Series, USA, 1992.
[35] Kells, L. *Elementary Differential Equations.* 6th ed., McGraw Hill Kogakusho Ltd., 1965.